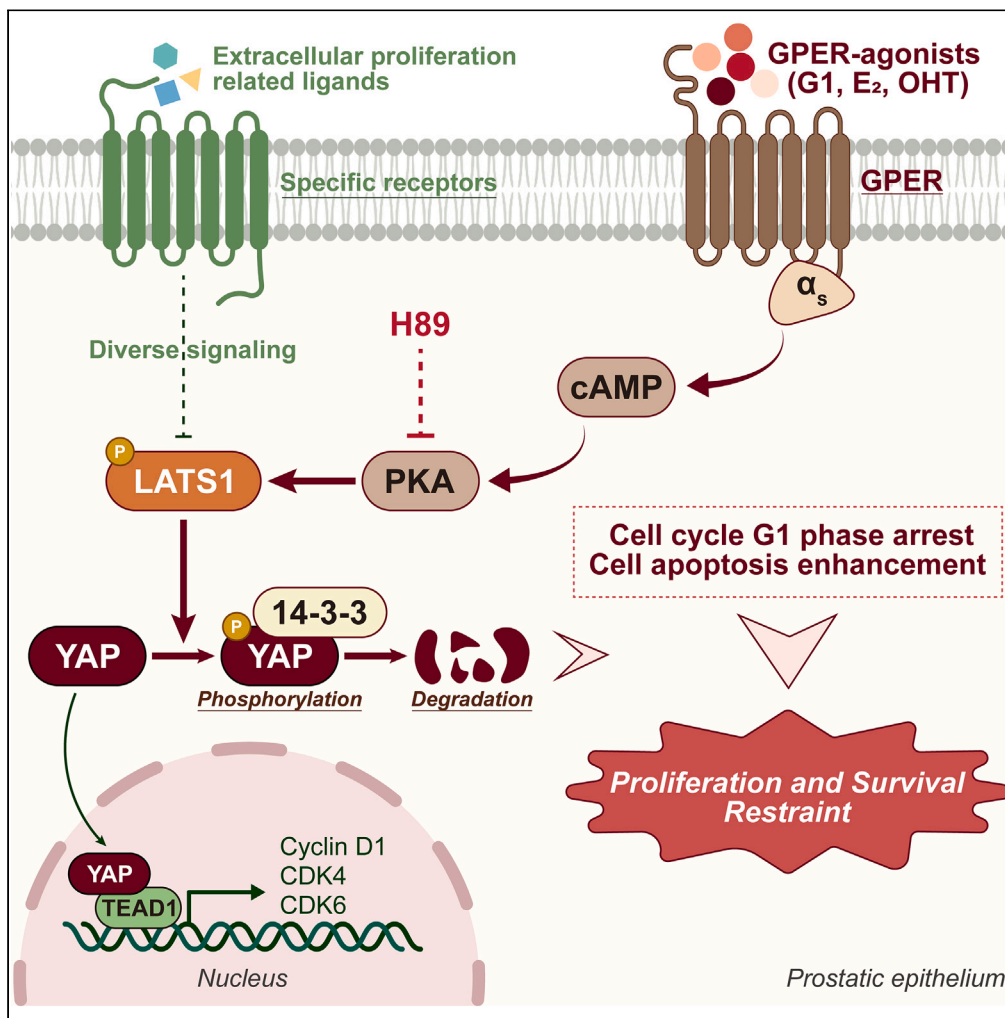


Article

# YAP-mediated GPER signaling impedes proliferation and survival of prostate epithelium in benign prostatic hyperplasia



Zhifu Liu, Senmao Li, Shengbin Chen, ..., Wei Liu, Shuai Hu, Jie Jin

hushuai926@bjmu.edu.cn (S.H.)  
jinjie@vip.163.com (J.J.)

Highlights

Epithelium-rich BPH tissues possess more YAP, less GPER and lower estrogen

Restraint of YAP inhibits cell proliferation and induces cell apoptosis

GPER activation enhances the phosphorylation and degradation of YAP

$G\alpha_s$ /cAMP/PKA activates LATS1 post-GPER, leading to YAP degradation



## Article

## YAP-mediated GPER signaling impedes proliferation and survival of prostate epithelium in benign prostatic hyperplasia

Zhifu Liu,<sup>1,2,3,9</sup> Senmao Li,<sup>1,2,3,4,9</sup> Shengbin Chen,<sup>1,2,3,9</sup> Jindong Sheng,<sup>1,2,3,5,9</sup> Zheng Li,<sup>1,2,3</sup> Tianjing Lv,<sup>1,2,3</sup> Wei Yu,<sup>1,2,3</sup> Yu Fan,<sup>1,2,3</sup> Jinlong Wang,<sup>6</sup> Wei Liu,<sup>7,8</sup> Shuai Hu,<sup>1,2,3,\*</sup> and Jie Jin<sup>1,2,3,4,8,10,\*</sup>

## SUMMARY

**Benign prostatic hyperplasia (BPH) occurs when there is an imbalance between the proliferation and death of prostate cells, which is regulated tightly by estrogen signaling. However, the role of G protein-coupled estrogen receptor (GPER) in prostate cell survival remains ambiguous. In this study, we observed that prostates with epithelial hyperplasia showed increased yes-associated protein 1 (YAP) expression and decreased levels of estrogen and GPER. Blocking YAP through genetic or drug interventions led to reduced proliferation and increased apoptosis in the prostate epithelial cells. Interestingly, GPER agonists produced similar effects. GPER activation enhanced the phosphorylation and degradation of YAP, which was crucial for suppressing cell proliferation and survival. The *Gαs*/cAMP/PKA/LATS pathway, downstream of GPER, transmitted signals that facilitated YAP inhibition. This study investigated the interaction between GPER and YAP in the prostate epithelial cells and its contribution to BPH development. It lays the groundwork for future research on developing BPH treatments.**

## INTRODUCTION

As the world population ages, the incidence and prevalence of benign prostatic hyperplasia (BPH) have rapidly increased.<sup>1</sup> Histologically, BPH is characterized by an increased number of epithelial and stromal cells in the periurethral area of the prostate.<sup>2</sup> Alterations of the balance between cell proliferation versus cell death owing to steroid hormones are considered to be a cause of BPH. And multiple lines of evidence support a role for estrogens in BPH pathogenesis to date.<sup>3</sup>

Estrogen has been reported to promote the proliferation of prostate stromal cells and inhibit epithelial cell proliferation both *in vitro* and *in vivo*, which is attributed to the classical nuclear estrogen-responsive receptors ER $\alpha$  and ER $\beta$ .<sup>4–9</sup> Additionally, GPER (G protein-coupled estrogen receptor) significantly modulates cell proliferation and apoptosis.<sup>10,11</sup> It recently became clear to us that GPER signaling plays a role in the growth and development of the prostate. High GPER expression in prostate basal epithelial cells has been revealed,<sup>12</sup> and selective GPER stimulation by G1 suppresses prostate cell (BPH-1,<sup>13</sup> RWPE-1,<sup>14</sup> and WPMY-1<sup>15</sup> cells) proliferation and arrests the cell cycle. The activation of GPER/ERK pathway and subsequent upregulation of p53 and p21 and down-regulation of cyclin D1 in human prostate stromal cell line WPMY-1 was shown to inhibit proliferation.<sup>15</sup> Yang. et al. recently demonstrated that GPER activation induces prostate epithelial cell apoptosis to relieve hyperplasia in a Ca<sup>2+</sup> mobilization-dependent manner.<sup>14</sup> However, downstream molecular alterations in prostatic epithelia after GPER activation during BPH development have yet to be elucidated.

In this study, the liquid chromatography-tandem mass spectrometry (LC-MS/MS) analysis found that BPH tissues predominated by epithelia showed lower estrogen content, weaker GPER expression but a higher expression of yes-associated protein 1 (YAP). YAP, along with its homolog TAZ, are two downstream transcription coactivators and the core components of the Hippo signaling pathway.<sup>16</sup> The Hippo signaling pathway is an evolutionarily conserved pathway from *Drosophila* to mammals and serves as a key regulator of tissue growth and

<sup>1</sup>Department of Urology, Peking University First Hospital, Beijing 100034, China

<sup>2</sup>Institute of Urology, Peking University, Beijing 100034, China

<sup>3</sup>Beijing Key Laboratory of Urogenital Diseases (Male), Molecular Diagnosis and Treatment Center, National Research Center for Genitourinary Oncology, Beijing 100034, China

<sup>4</sup>Department of Urology, Peking University Shenzhen Hospital, Shenzhen 518036, China

<sup>5</sup>Department of Gynaecological Oncology, Tianjin Medical University Cancer Institute and Hospital, National Clinical Research Center for Cancer, Key Laboratory of Cancer Prevention and Therapy of Tianjin, Tianjin's Clinical Research Center for Cancer, Tianjin 300060, China

<sup>6</sup>Department of Urology, Tibet Autonomous Region People's Hospital, Lhasa 850000, China

<sup>7</sup>Shenzhen Key Laboratory for Neuronal Structural Biology, Biomedical Research Institute, Shenzhen 518036, China

<sup>8</sup>Shenzhen Peking University-The Hong Kong University of Science and Technology Medical Center, Shenzhen 518036, China

<sup>9</sup>These authors contributed equally

<sup>10</sup>Lead contact

\*Correspondence: hushuai926@bjmu.edu.cn (S.H.), jinjie@vip.163.com (J.J.)

<https://doi.org/10.1016/j.isci.2024.109125>



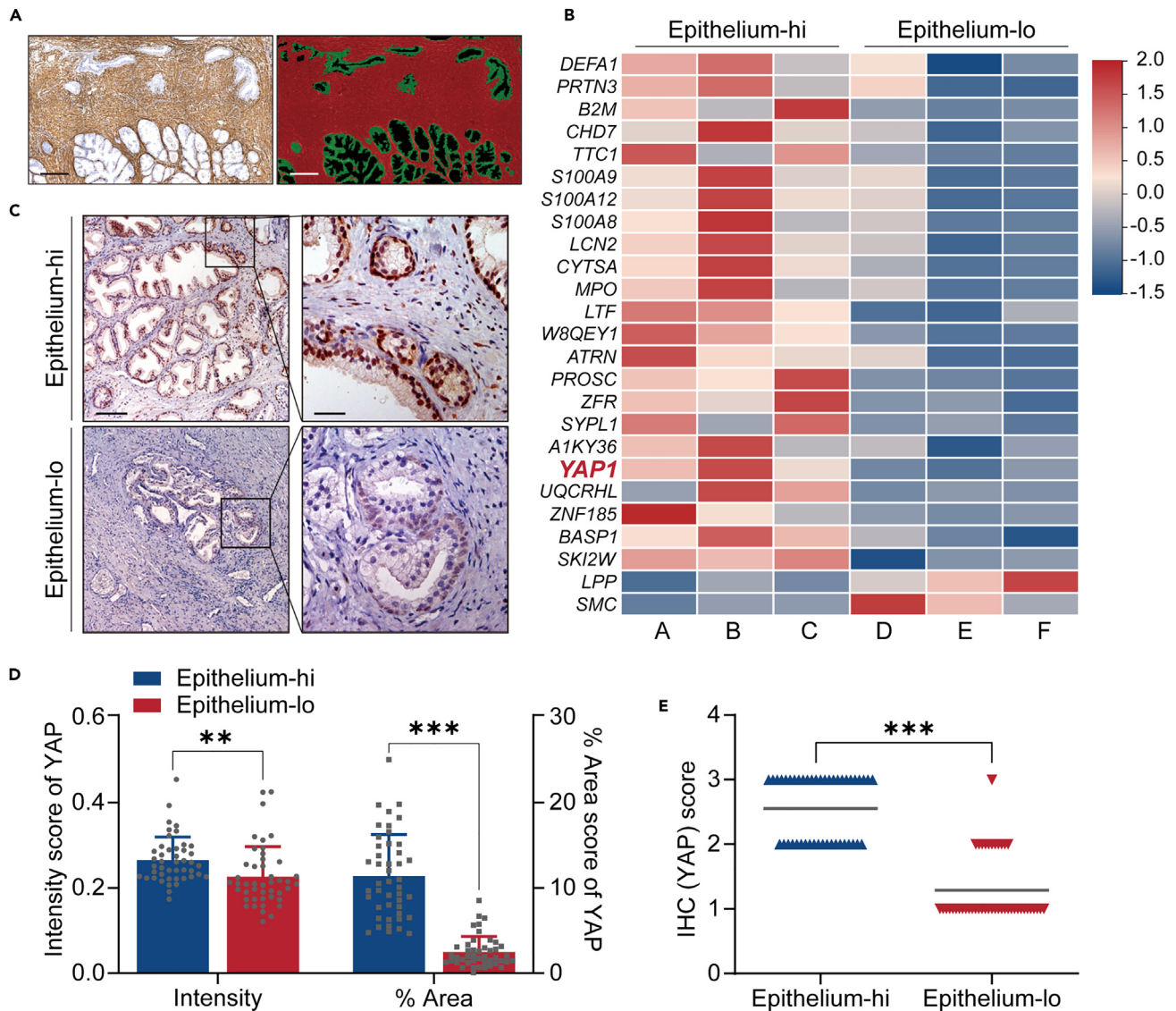


**Figure 1. YAP expression is elevated in epithelium-rich BPH group**

(A) Left: Representative staining of  $\alpha$ -SMA in BPH tissue. Right: Analysis of the same tissue specimen showing epithelial and stromal components using the Strata Quest Histo system (stroma in red, epithelia in green; Scale bars: 100  $\mu$ m).

(B) Heatmap illustrating the differentially expressed proteins in BPH tissues from Epithelium-hi compared to Epithelium-lo, including YAP.

(C) Representative immunohistochemical staining for YAP in Epithelium-hi and Epithelium-lo BPH tissues, demonstrating distinct expression patterns (Scale bars: 100  $\mu$ m [left]; 25  $\mu$ m [right]).

(D) Scatterplot depicting the variation in YAP staining intensity and area within epithelial cells between the Epithelium-hi and Epithelium-lo groups.

(E) Comparative scores of epithelial YAP expression in the two groups (0 = lowest, 3 = highest), showing significantly higher YAP expression in the epithelial cells of the Epithelium-hi group. Data were presented as mean  $\pm$  SD (n = 45). Significant difference was determined by two-tailed unpaired t test (D) or Mann-Whitney test (E) (\*\*p < 0.01, \*\*\*p < 0.001).

organ size by influencing cell proliferation and apoptosis.<sup>17–19</sup> YAP on and off drive distinct cell phenotype profiles, especially in various cancers.<sup>20</sup> Recent studies have also implied that the Hippo/YAP pathway is actively regulated by estrogens and their corresponding receptors. Zhou. et al. reported that the Hippo/YAP signaling pathway is a key downstream signaling branch of the GPER pathway and plays a critical role in breast cancer cell proliferation and tumor growth.<sup>21</sup>

These observations raise the possibility that the interactions between estrogen, estrogenic receptors and YAP may exert an influence on the proliferation-apoptosis balance of prostatic epithelial cell. In the present study, we investigated the crosstalk between GPER and YAP in the prostatic epithelia, and explored its role in BPH pathogenesis.

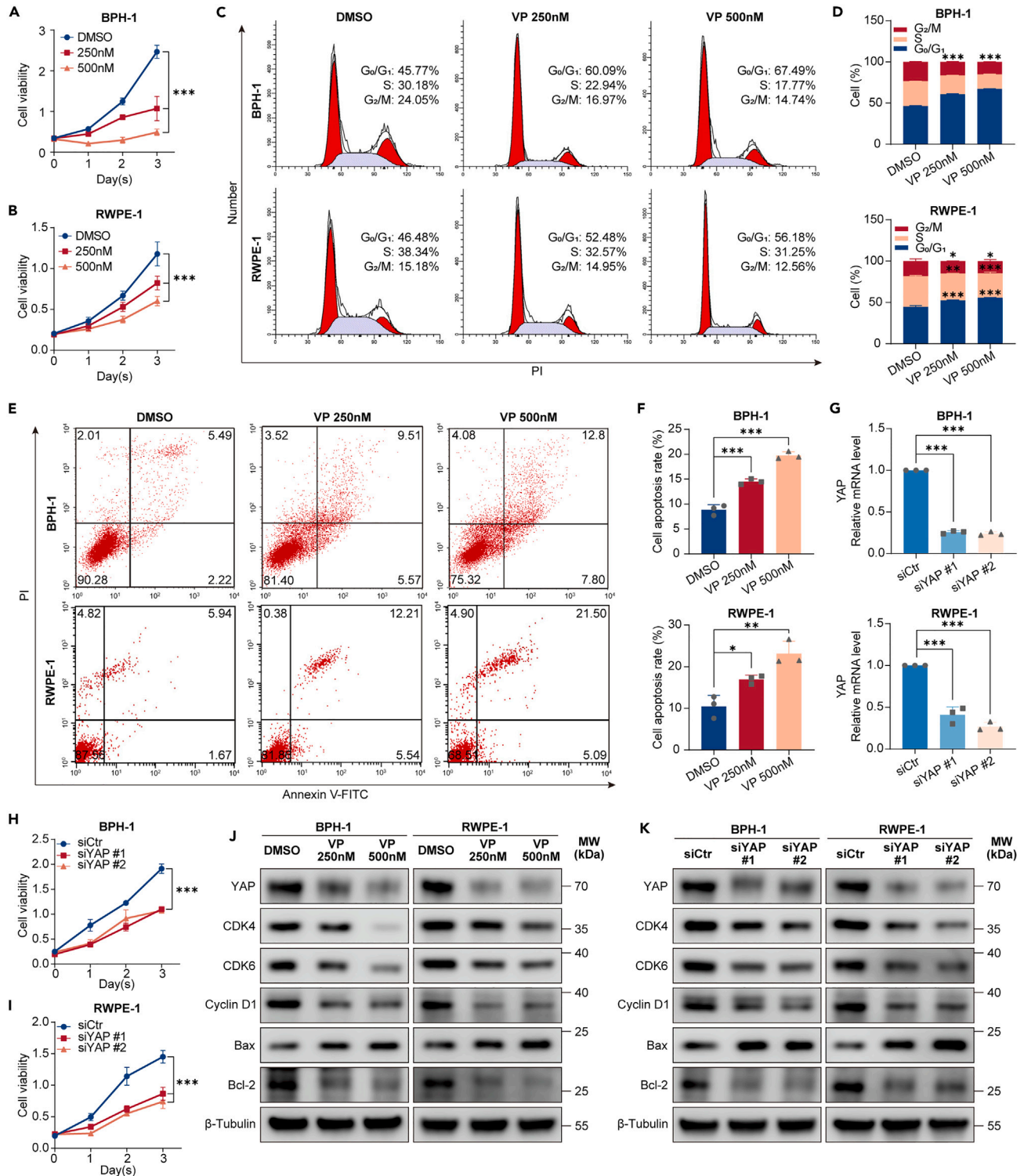


**Figure 2. Restraint of YAP inhibits cell proliferation and induces cell apoptosis**

(A–F) BPH-1 and RWPE-1 cell lines were subjected to either DMSO treatment or indicated concentrations of verteporfin. (A and B): Cell growth dynamics of both cell lines were monitored through CCK-8 assays conducted at 24-h intervals. (C and D): After 48 h, FCM analysis determined the distribution of cells across different cell cycle phases, with the histograms representing the proportion of cells in each phase. (E and F): Cell apoptosis was assessed after 48 h using Annexin V-FITC/PI staining and FACS, with the histograms illustrating the apoptosis rates.

**Figure 2. Continued**

(G) The efficacy of siRNAs targeting YAP was evaluated using RT-qPCR, with GAPDH serving as the endogenous control.

(H and I) Post-RNAi knockdown of YAP in both cell lines, cell growth curves were charted using CCK-8 assays at 24-h intervals.

(J and K) Western blot analysis was conducted to measure the relative expression levels of YAP, CDK4/6, cyclin D1, Bax, and Bcl-2 following either verteporfin treatment or RNAi intervention.  $\beta$ -Tubulin was used as a loading control. All blots shown are representative of three experimental replicates. Data are expressed as mean  $\pm$  SD from a minimum of three independent experiments. Significant difference was determined by one way ANOVA followed by a Tukey's multiple comparison tests (\* $p < 0.05$ , \*\* $p < 0.01$ , \*\*\* $p < 0.001$ ).

## RESULTS

### YAP expression is elevated in epithelium-rich BPH group

To investigate proteins potentially involved in the survival of prostate epithelial cells, we initially collected prostate tissues from 32 BPH patients (patient characteristics are detailed in [Table S1](#)). Subsequently, we conducted immunohistochemistry (IHC) staining using an anti-alpha-smooth muscle actin ( $\alpha$ -SMA) antibody, recognized as a marker for smooth muscle cells and myofibroblasts. We delineated the areas of the stroma, glandular epithelium, and glandular lumen based on this staining<sup>22</sup> ([Figure 1A](#)). We digitized and conducted subsequent analysis of the relative percentage of different tissue components, including the stroma/epithelium ratio (S/E). Specimens were ranked based on the S/E ratio, leading to the categorization of the 9 specimens with the lowest S/E into group 1 (Epithelium-hi), where the epithelial components may have more significant roles in BPH development. Conversely, the 9 specimens with the highest S/E were placed in group 2 (Epithelium-lo). Within each group, we further subdivided them into 3 subgroups labeled as A through E (details provided in [Table S1](#)). Subsequently, we employed isobaric tags for relative and absolute quantitation (iTRAQ)-based liquid chromatography-tandem mass spectrometry (LC-MS/MS) to identify the differentially expressed proteins (DEPs) between the two main groups. A total of 2,433 proteins were tested, resulting in the discovery of 25 DEPs ([Figure 1B](#)), among which YAP exhibited a 1.57-fold increase in expression in the Epithelium-hi group.

Because we collected the total protein from the mixture of stroma and epithelium, precise localization and quantification of YAP in each specimen became essential. Subsequent IHC staining of YAP revealed that it is predominantly expressed in the glandular epithelium. Further staining of Epithelium-hi and Epithelium-lo group demonstrated significantly stronger YAP staining in the epithelial cells of Epithelium-hi group ([Figures 1C and S1](#)). Statistical analysis of the 18 specimens confirmed that YAP levels were significantly higher in epithelial region of the Epithelium-hi group. There was Quantitative analysis revealed a significant difference in epithelial YAP staining intensity ( $p = 0.0024$ ) and area ( $p < 0.001$ ) between the two groups ([Figure 1D](#)). The IHC score of YAP in Epithelium-hi group was higher than the other ([Figure 1E](#)). Collectively, these findings suggest that YAP accumulated in the epithelia of epithelium-rich BPH group.

### Restraint of YAP inhibits cell proliferation and induces cell apoptosis

As previously reported, the Hippo-YAP signaling pathway plays a pivotal role in regulating the balance between cell proliferation and apoptosis.<sup>17,23</sup> However, the functionality of this pathway in the BPH prostatic epithelium remained unclear. Verteporfin (VP), a specific inhibitor of YAP, prevents its nuclear localization and disrupts its interaction with TEAD.<sup>24–26</sup> The Cell Counting Kit-8 (CCK-8) assay demonstrated that VP effectively inhibited the proliferation of both BPH-1 ([Figure 2A](#)) and RWPE-1 ([Figure 2B](#)) cells in a time- and dose-dependent manner ( $p < 0.001$ ). Both cell types exhibited impaired proliferation and an increased rate of apoptosis, potentially preventing cell accumulation. Consequently, flow cytometry (FCM) analysis was conducted to assess changes in cell proliferation and apoptosis following exposure to two different concentrations (250 and 500 nM) of VP for 48 h. We observed that the proportion of cells in the G<sub>0</sub>/G<sub>1</sub> phase increased, while that in the S phase decreased with increasing VP concentration in both cell lines, compared to the control group ([Figures 2C and 2D](#)). Additionally, the average percentage of apoptotic BPH-1 cells, as determined by Annexin V-FITC/PI staining, increased from  $8.85 \pm 1.01\%$  (DMSO) in the control group to  $14.51 \pm 0.56\%$  (VP 250 nM,  $p < 0.001$ ) and  $19.75 \pm 0.75\%$  (VP 500 nM,  $p < 0.001$ ) in the VP-treated groups. For the RWPE-1 cells, the rate of apoptosis also reached  $16.97 \pm 1.01\%$  (VP 250 nM,  $p < 0.05$ ) and  $23.15 \pm 2.98\%$  (VP 500 nM,  $p < 0.01$ ) following VP treatment ([Figures 2E and 2F](#)). Immunofluorescence staining ([Figure S2](#)) and immunoblotting ([Figure 2J](#)) confirmed a dose-dependent suppression of YAP's expression and nuclear localization by VP. Correspondingly, immunoblotting demonstrated a significant upregulation of the Bax/Bcl-2 expression ratio following VP treatment relative to the DMSO group. In contrast, the expression of proteins involved in cell cycle progression, such as CDK4, CDK6, and cyclin D1, was markedly diminished, thereby substantiating VP's role in G<sub>1</sub> phase arrest ([Figure 2J](#)).

Given that VP is an exogenous drug that inhibits the effect of YAP, we employed two small interfering RNAs (siRNAs) targeting YAP to further validate its role in prostate epithelial cell survival. The effectiveness of these siRNAs is illustrated in [Figure 2G](#). The CCK-8 assay yielded similar results to those observed following VP treatment. YAP knockdown significantly inhibited BPH-1 and RWPE-1 cell proliferation ([Figures 2H and 2I](#);  $p < 0.001$ ), impacting cell cycle progression and apoptosis ([Figure S3](#)). Similarly, immunoblotting revealed a downregulation in the expression of CDK4, CDK6, and cyclin D1, accompanied by an increased Bax/Bcl-2 ratio ([Figure 2K](#)). Collectively, these findings indicate that YAP plays a regulatory role in the proliferation and apoptosis of prostate epithelial cells.

### YAP expression is negatively related to tissue estrogen and GPER level

BPH is a hormone-dependent disease, hormonal alterations, particularly dynamic changes in androgen and estrogen levels, are crucial in BPH development.<sup>3</sup> Therefore, we conducted an additional LC-MS/MS analysis to examine the hormonal profiles of the 32 BPH tissues ([Table S1](#)), aiming to identify potential factors influencing YAP regulation, epithelium accumulation, and BPH development. A simple regression analysis was then conducted to assess the linear relationship between specific hormones and the S/E ratio. The results indicated that a higher S/E ratio

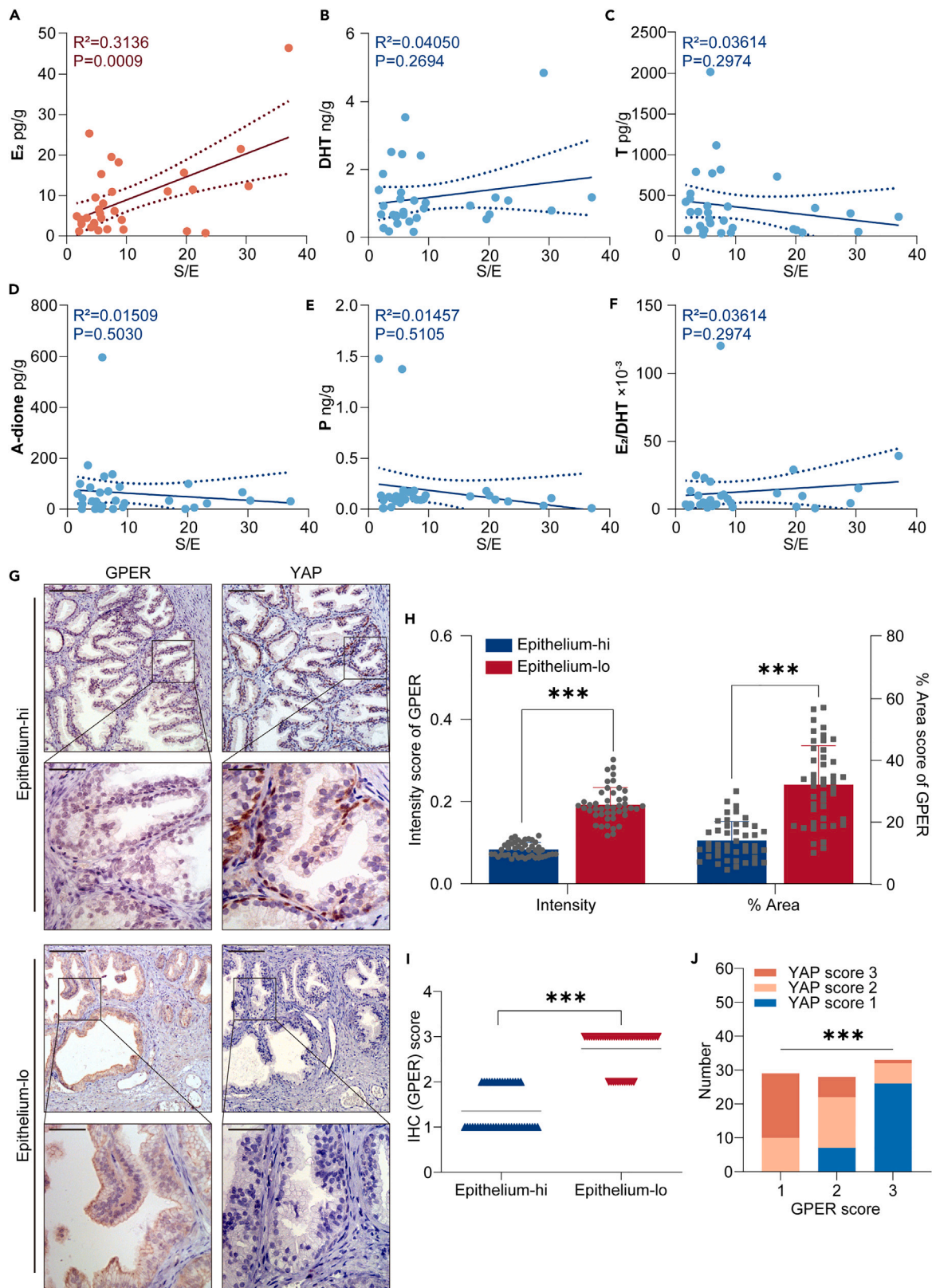


**Figure 3. YAP expression is negatively related to tissue estrogen and GPER level**

(A–F) These scatterplots display the levels of various hormones—17 $\beta$ -estradiol (E<sub>2</sub>), dihydrotestosterone (DHT), testosterone (T), androstenedione (A-dione), and progesterone (P)—in BPH specimens characterized by S/E ratios. Notably, a higher S/E ratio was positively correlated with increased levels of E<sub>2</sub> in the tissues (R = 0.3136, p < 0.001, n = 32). However, no significant correlation was observed between the S/E ratio and the concentrations of other hormones studied. (G) This panel shows consecutive histological sections of epithelial cells from the Epithelium-hi and Epithelium-lo groups, stained to reveal the expression of GPER and YAP, respectively (Scale bars: 100  $\mu$ m [up]; 25  $\mu$ m [down]). (H) A scatterplot illustrating the scores for epithelial GPER staining intensity and area in the Epithelium-hi and Epithelium-lo groups (n = 45). (I) Comparative scores of epithelial GPER expression in the two groups (0 = lowest, 3 = highest) (n = 45). (J) A negative correlation was observed between the expression of YAP and GPER in the epithelial cells. Data are expressed as mean  $\pm$  SD. Significant difference was determined by Pearson's correlation analysis (A–F), two-tailed unpaired t test (H), Mann-Whitney test (E), or Chi-square test (J) (\*\*p < 0.01, \*\*\*p < 0.001).

(suggesting less epithelium and reduced YAP expression) was positively correlated with 17 $\beta$ -estradiol (E<sub>2</sub>) levels in the tissues (R<sup>2</sup> = 0.5710, p < 0.001, Figure 3A). Conversely, no significant correlation was observed between the S/E ratio and other hormones, such as dihydrotestosterone (DHT), testosterone (T), androstenedione (A-dione), and progesterone (P) (Figures 3B–3E). Similarly, no correlation was found between the ratio of E<sub>2</sub> to DHT (E<sub>2</sub>/DHT) (Figure 3F), which has been previously reported to positively correlate with the proportion of stromal tissue.<sup>27</sup> These findings suggest that E<sub>2</sub> may have a negative impact on epithelial cell proliferation and survival.

Some recent studies have shown that the nonclassical estrogen-responsive receptor GPER is actively engaged in the regulation of YAP.<sup>21,28</sup> IHC staining was performed to analyze the expression of epithelial GPER in regions exhibiting varying YAP levels. This analysis demonstrated that GPER expression was markedly reduced in the YAP-accumulated epithelial cells of the Epithelium-hi group (Figures 3G and S1). In the Epithelium-hi group, both epithelial GPER staining intensity (p < 0.001) and area (p < 0.001) were significantly lower compared to the Epithelium-lo group (Figure 3H), as was the IHC score of GPER (Figure 3I). Subsequent statistical analysis revealed a negative correlation between epithelial YAP expression and GPER expression ( $\chi^2$  = 54.79, p < 0.001, Figure 3J). All of these observations led us to hypothesize that GPER-mediated estrogen signaling may suppress the expression and function of YAP in epithelial cells, disrupting cell proliferation and survival.

**Activation of GPER impedes the proliferation and survival of prostate epithelial cells**

To determine whether GPER activation affects the proliferation of BPH-1 and RWPE-1 cells, we treated these cells with G1, a selective GPER agonist that does not activate classic nuclear estrogen receptors (ERs).<sup>29</sup> Cell viability was assessed over four continuous days using the CCK-8 assay. We observed significant inhibition of BPH-1 cell proliferation when 1  $\mu$ M and 2.5  $\mu$ M G1 were applied (Figures 4A and 4C left panel, p < 0.001). Similarly, cell proliferation was inhibited following treatment with 10 nM and 100 nM E<sub>2</sub> (Figures 4A and 4C middle panel, p < 0.001). Additionally, the application of 5  $\mu$ M and 10  $\mu$ M 4-hydroxytamoxifen (OHT), an ER antagonist and GPER agonist,<sup>21</sup> mimicked the effects of G1 and VP (Figures 4A and 4C right panel, p < 0.001), suggesting that GPER activation alone could inhibit cell proliferation. Figure 4B depicts the results for RWPE-1 cells following G1 and E<sub>2</sub> treatment. To elucidate the mechanism underlying the inhibition of cell accumulation by these GPER agonists, we conducted FCM analysis, revealing cell cycle G1 phase arrest (Figures 4E and 4F) and increased apoptosis (Figures 4G and 4H), akin to the effects observed with VP treatment. To validate the role of GPER activation in prostate epithelial cell survival, we investigated the effects of G15, a G1 analog that preferentially inhibits GPER.<sup>30</sup> We discovered that G15 counteracted the cell proliferation inhibition induced by G1 and E<sub>2</sub> (Figure 4I). Moreover, the knockdown of GPER expression using siRNAs mitigated the effects of G1 on BPH-1 cells (Figure 4J). Additionally, immunoblotting revealed that G1 and E<sub>2</sub> treatment upregulated the Bax/Bcl-2 expression ratio while downregulating CDK4, CDK6, and cyclin D1 expression, indicating alterations in proteins related to cell cycle and apoptosis (Figure 4K). Similarly, G15 counteracted the protein expression changes induced by G1 treatment (Figure 4L). Our findings confirm that GPER activation impedes the proliferation and survival of prostate epithelial cells in BPH.

**GPER acts via inhibition of YAP**

To determine whether YAP influences GPER-induced cell proliferation impairment, we analyzed the expression of YAP and its homolog TAZ during the process. We observed that YAP and TAZ underwent significant phosphorylation and degradation in the presence of GPER agonists (E<sub>2</sub>, G1, and OHT) (Figure 5A). In contrast, the phosphorylation of YAP/TAZ was not promoted by the addition of G1 following G15 pre-treatment (Figure 5B). Consistent with these observations, GPER knockdown using siRNAs suppressed the effects of G1 on YAP degradation (Figure 5C). To exclude the effects of ERs, we examined the impact of E<sub>2</sub> on ER $\beta$ -knockdown BPH-1 cells, yielding results that supported the same conclusion (Figure 5D). To confirm the functional inhibition of YAP by GPER activation, we analyzed the expression of YAP target genes. We discovered that G1 and E<sub>2</sub> treatment significantly downregulated the mRNA levels of CTGF, CYR61, EDN1, EGR1, and ANKRD1 (Figure 5D). Phosphorylation of YAP promotes its binding to 14-3-3 proteins and cytoplasmic retention.<sup>18,19</sup> We observed that G1 significantly reduced total YAP expression and its nuclear translocation in BPH-1 cells, an effect that was largely reversed by G15 treatment (Figures 5E and 5F). Correspondingly, further co-immunoprecipitation (coIP) analyses revealed that GPER activation impeded the nuclear accumulation of YAP and its interaction with TEAD1 in BPH-1 cells (Figure 5G). In summary, GPER activation inhibits YAP by inducing its phosphorylation and cytoplasmic retention, and degradation.

To validate the role of YAP, we induced YAP overexpression in BPH-1 cells (Figure 5S). We observed that YAP overexpression markedly attenuated the effects of G1 and E<sub>2</sub> on cell proliferation (Figure 5H). Additionally, cell-cycle arrest (Figures 5I and 5J) and reduced survival (Figures 5K and 5L) induced by these GPER agonists were significantly alleviated. In line with these observations, immunoblotting

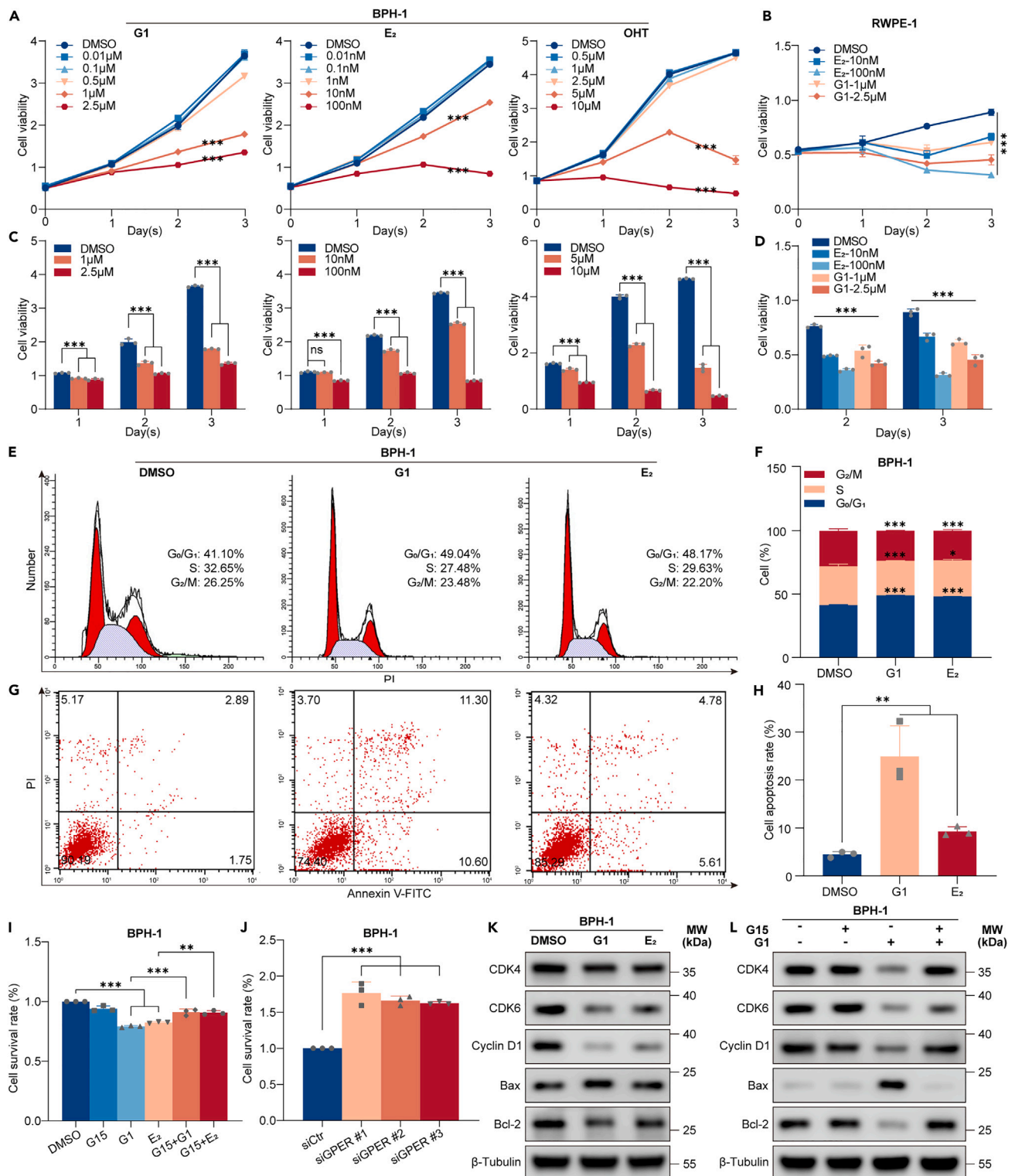


**Figure 4. Activation of GPER impedes the proliferation and survival of prostate epithelial cells**

(A and B) Growth curves for BPH-1 and RWPE-1 cell lines were established following treatment with G1, E2, or OHT at specified concentrations, using CCK-8 assays conducted every 24 h.

(C and D) Histograms illustrating cell viability on a daily basis with representative data.

**Figure 4. Continued**

(E and F) FCM assessed the distribution of cells across various cell cycle phases after 48 h of treatment with G1 (1  $\mu$ M) and E2 (10 nM). The histograms depict the proportion of cells in each specific phase.

(G and H) Cell apoptosis was evaluated using Annexin V-FITC/PI staining FACS following GPER activation by G1 and E2 treatments, with histograms illustrating the apoptosis rates.

(I) Pre-treatment with GPER blocker G15 (5  $\mu$ M) for 1 h mitigated the G1 and E2-induced inhibition of cell proliferation and survival. Cell survival rates were quantified using CCK-8 assays.

(J) GPER blockade via siRNA reduced the suppression of cell survival caused by G1, determined using CCK-8 assays.

(K) Western blot analysis was performed to determine the relative expression levels of CDK4/6, cyclin D1, Bax, and Bcl-2 post-treatment with G1 and E2.  $\beta$ -Tubulin was used as the loading control.

(L) The relative expression of aforementioned proteins was analyzed by western blot after pre-treatment with G15.  $\beta$ -Tubulin served as the loading control. All blots shown are representative of three experimental replicates. Data are expressed as mean  $\pm$  SD from a minimum of three independent experiments. Significant difference was determined by one way ANOVA followed by a Tukey's multiple comparison tests (\* $p < 0.05$ , \*\* $p < 0.01$ , \*\*\* $p < 0.001$ ).

demonstrated the reversal of the increased Bax/Bcl-2 ratio and the restoration of cell cycle progression-related proteins (Figure 5M) following YAP overexpression. Collectively, these findings led us to conclude that GPER activation impedes cell proliferation and survival through YAP deactivation in the prostate epithelium.

**GPER inhibits YAP through *G $\alpha$ s*/cAMP/PKA and LATS1 activation**

To assess whether GPER acts via MST and LATS kinases, key components of the Hippo pathway, in regulating YAP phosphorylation, we investigated the effect of G1 on the activities of MST1/2 and LATS1 kinases. We observed that G1 had no detectable effect on MST1/2 kinase activity. The ratio of phosphorylated MST (p-MST) to MST1 and MST2 was slightly reduced after G1 treatment (Figures 6A and 6B). Additionally, we measured the phosphorylation level of LATS1 (S909), a determinant of LATS activity, and found it to be notably increased following G1 treatment (Figures 6A and 6B). Previous studies suggested that LATS activation and YAP inhibition following GPCR activation might depend on the *G $\alpha$ s*/cAMP/PKA pathway,<sup>31</sup> in addition to the classic MST1/2 pathway. Coincidentally, we noted enhanced phosphorylation of the cAMP-responsive element-binding protein (CREB) (Figures 6A and 6B), implying that G1 stimulated *G $\alpha$ s* and cAMP production. Furthermore, inhibition of PKA using H 89 2HCl (H89)<sup>32</sup> alleviated the G1-induced reduction in YAP/TAZ and upregulation of p-LATS1, LATS1 (Figure 6C). Concurrently, pre-treatment with H89 reversed the G1-induced reduction in YAP expression and nuclear translocation (Figures 6D and 6E). Moreover, cell-cycle arrest (Figures 6F and 6G upper) and apoptosis (Figures 6F and 6G lower) induced by G1 were significantly mitigated when cells were pre-treated with H89. Collectively, these data confirm the role of the *G $\alpha$ s*/cAMP/PKA pathway in GPER activation-induced YAP phosphorylation and degradation, as well as in the restriction of cell survival in the prostate epithelium.

**DISCUSSION**

A critical factor in the development and progression of BPH is the disruption in the balance between cell proliferation and death, which allows proliferative processes to predominate. In this study, we discovered a protective role for GPER in epithelial hyperplasia, where GPER-mediated estrogen signaling effectively limited prostate epithelial cell proliferation and induced cell apoptosis through YAP inhibition. Our data also demonstrated that the *G $\alpha$ s*/cAMP/PKA pathway acted downstream of GPER to stimulate LATS kinase, promoting YAP phosphorylation and degradation. As such, our findings may serve as a foundation for future studies aimed at developing therapeutic interventions for BPH.

In the present study, the underlying molecular mechanisms of GPER-mediated indirect genomic signaling of estrogen in prostate epithelial cell survival and the pathogenesis of BPH were explored, and a more comprehensive understanding of GPER in YAP regulation was established. The estrogenic response in the prostate was determined by the type of ER present within prostate cells. Different actions may be mediated by stromal ER $\alpha$  and epithelial ER $\beta$ .<sup>3</sup> Prior evidence had indicated a controversial role for estrogen in BPH development. On the one hand, estrogen promotes BPH-derived primary prostate stromal cell proliferation via ER $\alpha$ <sup>4,6,8</sup>; on the other hand, prostate epithelial cells are induced to undergo apoptosis upon ER $\beta$  stimulation,<sup>9</sup> but selectively blocking ER $\beta$  only ameliorates this effect partially,<sup>14,33</sup> indicating a complicated mechanism is involved. Traditionally, estrogen is known to act through two classical transcription factors, ER $\alpha$  and ER $\beta$ , which mediate the genomic effects of estrogen,<sup>3</sup> but very little is known about the GPER in prostate. It is believed that GPER directly mediates or contributes to many of the rapid effects of estrogen in prostate. A recent study verified that GPER activation triggers Ca<sup>2+</sup> release from the endoplasmic reticulum of prostate epithelial cells, which increases the mitochondrial Ca<sup>2+</sup> concentration and thus induces cell apoptosis.<sup>14</sup> However, this commonly used model has been challenged since GPER has been documented to participate in the genomic effects of estrogen.<sup>21,34</sup> And our newly reported work has revealed a pro-proliferation and pro-fibrosis role of GPER signaling via EGFR/ERK and HIF-1 $\alpha$ /TGF- $\beta$ 1 signaling in prostatic stromal cell during BPH progression.<sup>35</sup> The observations that the expression of YAP was negatively correlated with the tissue estrogen content and GPER expression in epithelia of BPH specimens support a model of YAP deactivation by GPER in clinical samples. In this study, we confirmed that estrogen and G1 induced YAP phosphorylation and repressed their nuclear accumulation, diminishing the interaction between YAP and the transcription factor TEAD1. All of these findings implied a crucial role for the YAP pathway in mediating the genomic effects of GPER. Thus, we promote the understanding of the function of estrogen, especially the GPER-mediated signaling in prostate epithelial cell survival. GPER, together with YAP may be potential biomarkers for the epithelium-rich phenotype of BPH.

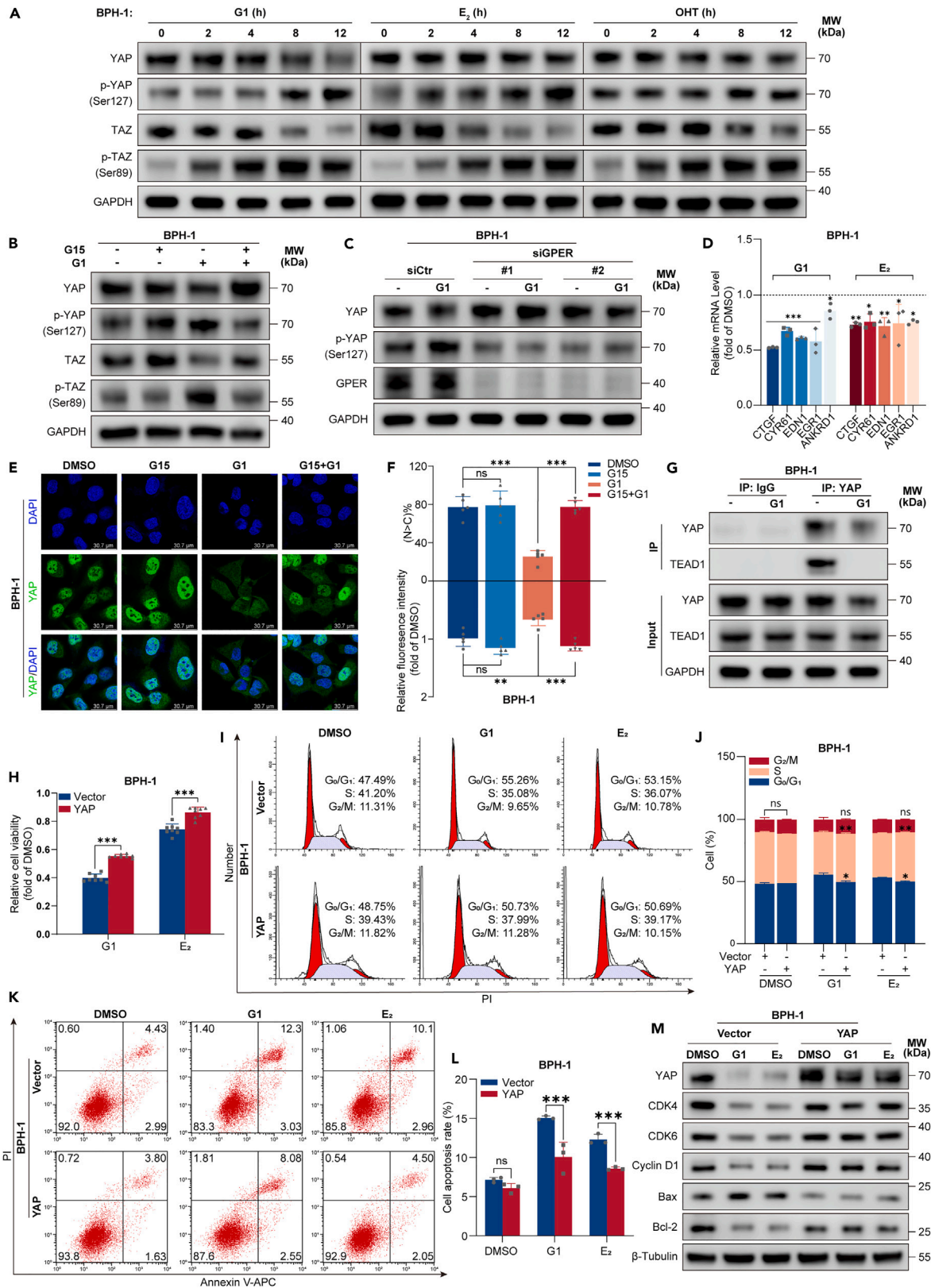


**Figure 5. GPER acts via inhibition of YAP**

(A) GPER activation led to the phosphorylation of YAP in BPH-1 cells treated with 1  $\mu$ M G1, 10 nM E2, or 5  $\mu$ M OHT. Immunoblotting was utilized to assess the relative expression levels of p-YAP/YAP, p-TAZ/TAZ, with GAPDH serving as the loading control. (B and C) GPER mediated YAP phosphorylation. GPER was inhibited by 5  $\mu$ M G15 pre-treatment (B) or siRNAs (C). Following this, BPH-1 cells were treated with G1, and immunoblotting was conducted to analyze the phosphorylation levels. (D) Activation of GPER suppressed the expression of YAP-induced target genes. BPH-1 cells treated with G1 or E2 for 24 h were subjected to quantitative PCR to measure mRNA levels of specific target genes. (E and F) G1 suppressed YAP's expression and nuclear localization. BPH-1 cells were treated with G1, with or without G15 pre-treatment. Immunofluorescence staining for YAP was performed, and quantifications of YAP's subcellular localization and staining intensity were done based on 5 randomly selected fields. N indicates nuclear localization; C indicates cytoplasmic. (G) GPER activation hindered the nuclear translocation of YAP and its interaction with TEAD1 in BPH-1 cells. After 24 h of G1 treatment, cells were subjected to immunoprecipitation using an anti-YAP antibody, followed by detection of coimmunoprecipitated TEAD1. (H–M) YAP was required for GPER to impede the proliferation and survival of prostate epithelial cells. (H): Overexpression of YAP significantly diminished the impact of G1 and E2 on cell proliferation, as determined by the CCK-8 assay. (I and J): FCM was used to evaluate the distribution of cells across different cell cycle phases, with histograms indicating the proportion of cells in each phase. (K and L): Cell apoptosis was assessed using Annexin V-FITC/PI staining FACS, with histograms showing apoptosis rates. (M): Immunoblotting was performed to analyze the relative expression of YAP, CDK4/6, cyclin D1, Bax, and Bcl-2 following treatment with G1 and E2, both with and without YAP overexpression.  $\beta$ -Tubulin was used as the loading control. All blots shown are representative of three experimental replicates. Data are expressed as mean  $\pm$  SD from a minimum of three independent experiments. Significant difference was determined by one way ANOVA followed by a Tukey's multiple comparison tests (D and F) and two-tailed unpaired t test (H, J, and L) (\*p < 0.05, \*\*p < 0.01, \*\*\*p < 0.001, ns for non-significant).

Since the three disparate ERs play distinct and perhaps opposing roles in BPH, it is possible that selective ER modulators may be useful therapeutic strategies. Recent attempt of ER $\beta$ -signaling pathway disruption failed to improve symptoms in men with BPH.<sup>33</sup> However, an antagonist of ER but agonist of GPER, OHT, the active metabolite of tamoxifen, suppressed the proliferation of normal human prostate epithelial and stromal cells *in vitro*.<sup>36,37</sup> Our work showed that OHT both inhibited the function of YAP and induced cell apoptosis, which emphasizes that GPER is a promising target in BPH management, especially in patients with high expression of GPER or YAP in the epithelium. Therefore, this study lays the foundations for further studies that may directly influence therapeutic development.

GPCRs are well-established upstream regulators of the Hippo/YAP pathway. YAP signaling is augmented by GPCR-induced Hippo pathway quiescence in most cases, especially in tumorigenesis.<sup>38</sup> However, the most important observation in the present study was inhibition of YAP following GPER stimulation. Phosphorylation of YAP was notably enhanced after G1 and E<sub>2</sub> treatment, resulting in degradation of the key protein. The role of G $\alpha_s$ , cAMP, and PKA in relaying signals was further verified. We attribute these differences to cell heterogeneity and the different coupling proteins. GPCRs can potentially modulate the phosphorylation states and activity of YAP via various G proteins. GPCRs coupled with G $\alpha_{12/13}$ , G $\alpha_{q/11}$ , or G $\alpha_{i/o}$  stabilize YAP,<sup>31,39,40</sup> but YAP expression is inhibited when GPCRs are coupled with G $\alpha_s$ ,<sup>41</sup> which mainly relies on cAMP/PKA and subsequent LATS activation.<sup>31</sup> Consistent with previous reports, GPER can modulate YAP both positively and negatively. Zhou. et al. reported that estrogen activates YAP and oncoproteins downstream of the Hippo pathway through GPER.<sup>21</sup> In contrast, the work from Corte and colleagues showed that GPER-mediated estrogen signaling hampers YAP activation, modulating the mechanical reprogramming of myofibroblast-like cells in the tumor microenvironment of hepatocellular carcinoma and pancreatic cancer.<sup>28,42</sup> Moreover, the interaction between GPER and cAMP/PKA has been extensively described with other models. For example, in breast cancer cells, the GPER/cAMP/PKA signaling axis triggers reprogramming of tumor energy metabolism, conferring tumor cells with multiple drug resistance.<sup>43</sup> Additionally, GPER mediates bone mesenchymal stem cell proliferation via the cAMP/PKA/p-CREB pathway and subsequently upregulates cyclin D1/CDK6 and the cyclin E1/CDK2 complex.<sup>44</sup> All of these findings confirm a reliable role for the GPER/cAMP/PKA axis in YAP expression inhibition and help to establish a more comprehensive understanding of GPER in YAP regulation.

YAP is considered a key regulator of organ growth during mammalian development and regeneration.<sup>17</sup> And the crosstalk between YAP regulation and steroid hormones makes vast difference in various hormone-related diseases, such as breast cancer and prostate cancer.<sup>21,45</sup> Therefore, the role of YAP in BPH development and progression seems to be fairly attractive and significant. Previous reports have revealed that there is more epithelium as the size of the prostate increases,<sup>46,47</sup> indicating a potential role of epithelial cell proliferation in larger prostates. We found that epithelium-rich BPH tissues showed higher YAP expression and verified that genetic (RNAi) and pharmacological (verteporfin) disruption of YAP expression suppressed prostate epithelial cell proliferation and induced their apoptosis in BPH. Given human prostate is the only glandular organ that continues to undergo net growth as a man ages,<sup>48</sup> the YAP regulation may have important implications for the BPH development. However, future work is needed to clarify the relative contribution of YAP to prostate enlargement.

**Limitations of the study**

Although the present study has shown promising results regarding the inhibition of YAP and its downstream effects, there are still some unanswered questions regarding the underlying mechanism(s). Recent studies have suggested that the expression of CDK4, CDK6, and cyclin D1 is regulated directly or indirectly by YAP.<sup>49,50</sup> In line with these findings, our data demonstrated a potent inhibition of expression of these targets upon YAP phosphorylation and degradation, suggesting their potential involvement in the regulation of terminal cell cycle G1 arrest. Moreover, the study presents a reasonably convincing argument for the relevance of this pathway in the cell line; however, the investigation into its relevance *in vivo* is minimal, and the evidence provided is, at best, merely correlative. Therefore, future research should be directed

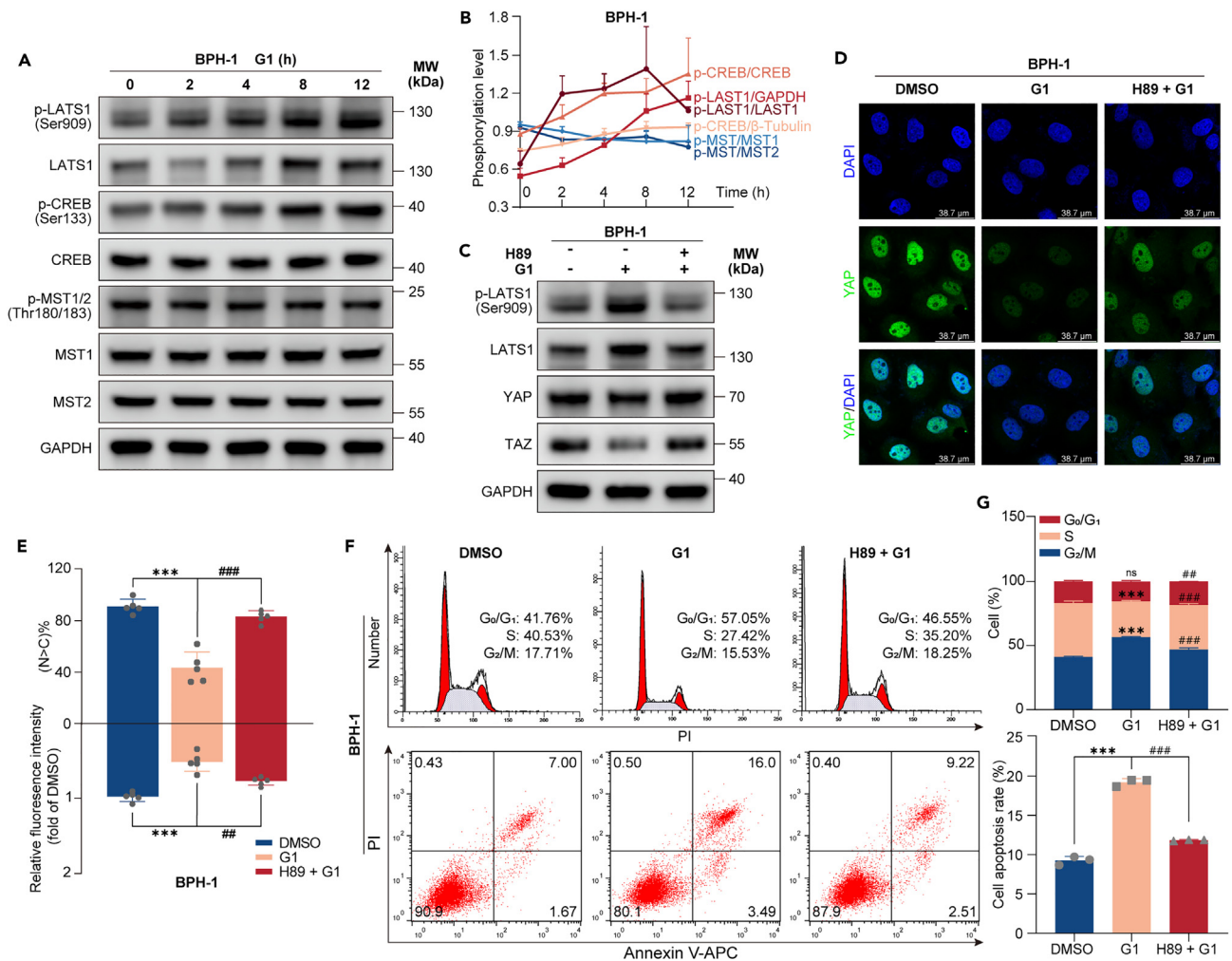


**Figure 6. GPER inhibits YAP through the  $G_{\alpha s}$ /cAMP/PKA pathway and LATS1 activation**

(A and B) Treatment of BPH-1 cells with 1  $\mu$ M G1 resulted in an elevation of phosphorylation levels for CREB and LATS1, whereas the phosphorylation levels of MST1/2 were either unchanged or exhibited a slight decrease. The cells were treated and collected at 2, 4, 8, and 12 h for immunoblotting to detect the phosphorylation levels of LATS, CREB, and MST1/2. The line chart depicts the time-dependent quantification of phosphorylation levels for CREB, LATS1, and MST1/2.

(C) PKA was required for G1 to inhibit YAP expression. BPH-1 cells pre-treated with 10  $\mu$ M PKA inhibitor H89 for 1 h underwent immunoblotting to assess the phosphorylation level of LATS1 and the expression levels of YAP and TAZ.

(D and E) Pre-treatment with H89 mitigated the G1-induced reduction in YAP expression and its nuclear localization. BPH-1 cells were treated with G1, with or without H89 pre-treatment, followed by immunofluorescence staining for YAP. Quantifications of YAP's subcellular localization and staining intensity were conducted from 5 randomly selected fields. N indicates nuclear localization; C indicates cytoplasmic.

(F and G) Blockade of PKA activity by pre-treatment with 10  $\mu$ M H89 for 1 h counteracted the G1-induced cell-cycle arrest (upper) and apoptosis (lower). Histograms display the proportion of cells in each cell cycle phase and the apoptosis rates. All blots shown are representative of three experimental replicates. Data are expressed as mean  $\pm$  SD from a minimum of three independent experiments. Significant difference was determined by one way ANOVA followed by a Tukey's multiple comparison tests (\*\* $p < 0.001$  compared with DMSO treatment; ## $p < 0.01$ , ### $p < 0.001$  compared with G1 treatment, ns for non-significant).

toward exploring how YAP mediates changes in molecules crucial for prostatic epithelial proliferation and apoptosis. Additionally, conducting treatment studies in animal models would be a valuable extension of this work.

## STAR METHODS

Detailed methods are provided in the online version of this paper and include the following:

- KEY RESOURCES TABLE

- **RESOURCE AVAILABILITY**
  - Lead contact
  - Materials availability
  - Data and code availability
- **EXPERIMENTAL MODEL AND STUDY PARTICIPANT DETAILS**
  - Patients and tissue samples
  - Cell culture and transfection
- **METHOD DETAILS**
  - iTRAQ-based LC-MS/MS
  - Hormone analysis
  - Immunohistochemistry and immunofluorescence
  - RNAi
  - RNA extraction and quantitative real-time PCR (qRT-PCR)
  - Western blot analysis
  - CCK-8 cell proliferation assay
  - Flow cytometry analysis
- **QUANTIFICATION AND STATISTICAL ANALYSIS**

## SUPPLEMENTAL INFORMATION

Supplemental information can be found online at <https://doi.org/10.1016/j.isci.2024.109125>.

## ACKNOWLEDGMENTS

We would like to express our gratitude to all those who financed the subject. This research was supported by grants from the National Natural Science Foundation of China (No. 82070777 and 82270808), Shenzhen Basic Research Grants (No. JCYJ20190813094201662 and JCYJ20220531093006014), Natural Science Foundation of Guangdong Province, China (No. 2021A1515010810) to J.J.; Tibetan Natural Science Foundation (No. XZ2019ZR-ZY16(Z)) to Y.F.; Guangdong Basic and Applied Basic Research Fund-Joint Fund Project (Youth Fund-2021A1515111141) and the Scientific Research Foundation of Peking University Shenzhen Hospital (No. KYQD2021086) to S.L.; National Natural Science Foundation of China (No. 31870746), Shenzhen Basic Research Grants (No. JCYJ20200109140414636), and Natural Science Foundation of Guangdong Province, China (No. 2021A1515010796) to W.L..

## AUTHOR CONTRIBUTIONS

J.Jin, S.Hu, and J.Sheng conceived and designed this study. Z.Liu, S.Li, S.Chen, J.Sheng, Z.Li, and T.Lv participated in laboratory work and performed the data analysis. Z.Liu, S.Li, and S.Chen wrote the original draft of the manuscript. W.Yu and J.Wang provided with clinical assistance and insights during the study. Y.Fan, W.Liu, S.Hu, and J.Jin participated in advising and revising the manuscript critically. J.Jin, W.Liu, Y.Fan, and S.Li provided the financial support. All authors reviewed and approved the manuscript.

## DECLARATION OF INTERESTS

The authors declare no competing interests.

Received: September 13, 2023

Revised: December 21, 2023

Accepted: January 31, 2024

Published: February 5, 2024

## REFERENCES

1. Chughtai, B., Forde, J.C., Thomas, D.D.M., Laor, L., Hossack, T., Woo, H.H., Te, A.E., and Kaplan, S.A. (2016). Benign prostatic hyperplasia. *Nat. Rev. Dis. Primers* *2*, 16031. <https://doi.org/10.1038/nrdp.2016.31>.
2. Roehrborn, C.G. (2008). Pathology of benign prostatic hyperplasia. *Int. J. Impot. Res.* *20*, S11–S18. <https://doi.org/10.1038/ijir.2008.55>.
3. Ho, C.K.M., and Habib, F.K. (2011). Estrogen and androgen signaling in the pathogenesis of BPH. *Nat. Rev. Urol.* *8*, 29–41. <https://doi.org/10.1038/nrurol.2010.207>.
4. Ho, C.K.M., Nanda, J., Chapman, K.E., and Habib, F.K. (2008). Oestrogen and benign prostatic hyperplasia: effects on stromal cell proliferation and local formation from androgen. *J. Endocrinol.* *197*, 483–491. <https://doi.org/10.1677/JOE-07-0470>.
5. Zhang, Z., Duan, L., Du, X., Ma, H., Park, I., Lee, C., Zhang, J., and Shi, J. (2008). The proliferative effect of estradiol on human prostate stromal cells is mediated through activation of ERK. *Prostate* *68*, 508–516. <https://doi.org/10.1002/pros.20722>.
6. Park, I.I., Zhang, Q., Liu, V., Kozlowski, J.M., Zhang, J., and Lee, C. (2009). 17Beta-estradiol at low concentrations acts through distinct pathways in normal versus benign prostatic hyperplasia-derived prostate stromal cells. *Endocrinology* *150*, 4594–4605. <https://doi.org/10.1210/en.2008-1591>.
7. King, K.J., Nicholson, H.D., and Assinder, S.J. (2006). Effect of increasing ratio of estrogen: androgen on proliferation of normal human prostate stromal and epithelial cells, and the malignant cell line LNCaP. *Prostate* *66*, 105–114. <https://doi.org/10.1002/pros.20327>.
8. Collins, A.T., Zhiming, B., Gilmore, K., and Neal, D.E. (1994). Androgen and oestrogen responsiveness of stromal cells derived from the human hyperplastic prostate: oestrogen

- regulation of the androgen receptor. *J. Endocrinol.* 143, 269–277. <https://doi.org/10.1677/joe.0.1430269>.
- McPherson, S.J., Hussain, S., Balanathan, P., Hedwards, S.L., Niranjani, B., Grant, M., Chandrasiri, U.P., Toivanen, R., Wang, Y., Taylor, R.A., and Risbridger, G.P. (2010). Estrogen receptor-beta activated apoptosis in benign hyperplasia and cancer of the prostate is androgen independent and TNFalpha mediated. *Proc. Natl. Acad. Sci. USA* 107, 3123–3128. <https://doi.org/10.1073/pnas.0905524107>.
  - Revankar, C.M., Cimino, D.F., Sklar, L.A., Arterburn, J.B., and Prossnitz, E.R. (2005). A transmembrane intracellular estrogen receptor mediates rapid cell signaling. *Science* 307, 1625–1630. <https://doi.org/10.1126/science.1106943>.
  - Prossnitz, E.R., and Barton, M. (2011). The G-protein-coupled estrogen receptor GPER in health and disease. *Nat. Rev. Endocrinol.* 7, 715–726. <https://doi.org/10.1038/nrendo.2011.122>.
  - Rago, V., Romeo, F., Giordano, F., Ferraro, A., and Carpino, A. (2016). Identification of the G protein-coupled estrogen receptor (GPER) in human prostate: expression site of the estrogen receptor in the benign and neoplastic gland. *Andrology* 4, 121–127. <https://doi.org/10.1111/andr.12131>.
  - Chan, Q.K.Y., Lam, H.M., Ng, C.F., Lee, A.Y.Y., Chan, E.S.Y., Ng, H.K., Ho, S.M., and Lau, K.M. (2010). Activation of GPR30 inhibits the growth of prostate cancer cells through sustained activation of Erk1/2, c-jun/c-fos-dependent upregulation of p21, and induction of G2 cell-cycle arrest. *Cell Death Differ.* 17, 1511–1523. <https://doi.org/10.1038/cdd.2010.20>.
  - Yang, D.L., Xu, J.W., Zhu, J.G., Zhang, Y.L., Xu, J.B., Sun, Q., Cao, X.N., Zuo, W.L., Xu, R.S., Huang, J.H., et al. (2017). Role of GPR30 in estrogen-induced prostate epithelial apoptosis and benign prostatic hyperplasia. *Biochem. Biophys. Res. Commun.* 487, 517–524. <https://doi.org/10.1016/j.bbrc.2017.04.047>.
  - Ren, G.Y., Chen, C.Y., Chen, W.G., Huang, Y., Qin, L.Q., and Chen, L.H. (2016). The treatment effects of flaxseed-derived secoisolariciresinol diglycoside and its metabolite enterolactone on benign prostatic hyperplasia involve the G protein-coupled estrogen receptor 1. *Appl. Physiol. Nutr. Metab.* 41, 1303–1310. <https://doi.org/10.1139/apnm-2016-0332>.
  - Piccolo, S., Dupont, S., and Cordenonsi, M. (2014). The biology of YAP/TAZ: hippo signaling and beyond. *Physiol. Rev.* 94, 1287–1312. <https://doi.org/10.1152/physrev.00005.2014>.
  - Yu, F.X., Zhao, B., and Guan, K.L. (2015). Hippo Pathway in Organ Size Control, Tissue Homeostasis, and Cancer. *Cell* 163, 811–828. <https://doi.org/10.1016/j.cell.2015.10.044>.
  - Dong, J., Feldmann, G., Huang, J., Wu, S., Zhang, N., Comerford, S.A., Gayyed, M.F., Anders, R.A., Maitra, A., and Pan, D. (2007). Elucidation of a universal size-control mechanism in Drosophila and mammals. *Cell* 130, 1120–1133. <https://doi.org/10.1016/j.cell.2007.07.019>.
  - Zhao, B., Wei, X., Li, W., Udan, R.S., Yang, Q., Kim, J., Xie, J., Ikenoue, T., Yu, J., Li, L., et al. (2007). Inactivation of YAP oncoprotein by the Hippo pathway is involved in cell contact inhibition and tissue growth control. *Genes Dev.* 21, 2747–2761. <https://doi.org/10.1101/gad.1602907>.
  - Pearson, J.D., Huang, K., Pacal, M., McCurdy, S.R., Lu, S., Aubry, A., Yu, T., Wadosky, K.M., Zhang, L., Wang, T., et al. (2021). Binary pancreatic cancer classes with distinct vulnerabilities defined by pro- or anti-cancer YAP/TEAD activity. *Cancer Cell* 39, 1115–1134. <https://doi.org/10.1016/j.ccell.2021.06.016>.
  - Zhou, X., Wang, S., Wang, Z., Feng, X., Liu, P., Lv, X.B., Li, F., Yu, F.X., Sun, Y., Yuan, H., et al. (2015). Estrogen regulates Hippo signaling via GPER in breast cancer. *J. Clin. Invest.* 125, 2123–2135. <https://doi.org/10.1172/JCI79573>.
  - Shapiro, E., Hartanto, V., and Lepor, H. (1992). Quantifying the Smooth Muscle Content of the Prostate Using Double-Immunoenzymatic Staining and Color Assisted Image Analysis. *J. Urol.* 147, 1167–1170. [https://doi.org/10.1016/s0022-5347\(17\)37508-0](https://doi.org/10.1016/s0022-5347(17)37508-0).
  - Shi, Y., Cao, T., Sun, Y., Xia, J., Wang, P., and Ma, J. (2019). Nitidine Chloride inhibits cell proliferation and invasion via downregulation of YAP expression in prostate cancer cells. *Am. J. Transl. Res.* 11, 709–720.
  - Liu-Chittenden, Y., Huang, B., Shim, J.S., Chen, Q., Lee, S.J., Anders, R.A., Liu, J.O., and Pan, D. (2012). Genetic and pharmacological disruption of the TEAD-YAP complex suppresses the oncogenic activity of YAP. *Genes Dev.* 26, 1300–1305. <https://doi.org/10.1101/gad.192856.112>.
  - Wang, C., Zhu, X., Feng, W., Yu, Y., Jeong, K., Guo, W., Lu, Y., and Mills, G.B. (2016). Verteporfin inhibits YAP function through up-regulating 14-3-3 $\sigma$  sequestering YAP in the cytoplasm. *Am. J. Cancer Res.* 6, 27–37.
  - Salem, O., Jia, S., Qian, B.-Z., and Hansen, C.G. (2023). AR activates YAP/TAZ differentially in prostate cancer. *Life Sci. Alliance* 6, e202201620. <https://doi.org/10.26508/lsa.202201620>.
  - Shibata, Y., Ito, K., Suzuki, K., Nakano, K., Fukabori, Y., Suzuki, R., Kawabe, Y., Honma, S., and Yamanaka, H. (2000). Changes in the endocrine environment of the human prostate transition zone with aging: simultaneous quantitative analysis of prostatic sex steroids and comparison with human prostatic histological composition. *Prostate* 42, 45–55. [https://doi.org/10.1002/\(sici\)1097-0045\(20000101\)42:1<45::aid-pros6>3.0.co;2-w](https://doi.org/10.1002/(sici)1097-0045(20000101)42:1<45::aid-pros6>3.0.co;2-w).
  - Cortes, E., Sarper, M., Robinson, B., Lachowski, D., Chronopoulos, A., Thorpe, S.D., Lee, D.A., and Del Rio Hernández, A.E. (2019). GPER is a mechanoregulator of pancreatic stellate cells and the tumor microenvironment. *EMBO Rep.* 20, e46556. <https://doi.org/10.15252/embr.201846556>.
  - Bologa, C.G., Revankar, C.M., Young, S.M., Edwards, B.S., Arterburn, J.B., Kiselyov, A.S., Parker, M.A., Tkachenko, S.E., Savchuck, N.P., Sklar, L.A., et al. (2006). Virtual and biomolecular screening converge on a selective agonist for GPR30. *Nat. Chem. Biol.* 2, 207–212. <https://doi.org/10.1038/nchembio775>.
  - Dennis, M.K., Burai, R., Ramesh, C., Petrie, W.K., Alcon, S.N., Nayak, T.K., Bologa, C.G., Leitao, A., Brailoiu, E., Deliu, E., et al. (2009). In vivo effects of a GPR30 antagonist. *Nat. Chem. Biol.* 5, 421–427. <https://doi.org/10.1038/nchembio.168>.
  - Yu, F.X., Zhao, B., Panupinthu, N., Jewell, J.L., Lian, I., Wang, L.H., Zhao, J., Yuan, H., Tumaneng, K., Li, H., et al. (2012). Regulation of the Hippo-YAP pathway by G-protein-coupled receptor signaling. *Cell* 150, 780–791. <https://doi.org/10.1016/j.cell.2012.06.037>.
  - Zhao, W.B., Lu, Q., Nguyen, M.N., Su, Y., Ziemann, M., Wang, L.N., Kiriazis, H., Puthalakath, H., Sadoshima, J., Hu, H.Y., and Du, X.J. (2019). Stimulation of beta-adrenoceptors up-regulates cardiac expression of galectin-3 and BIM through the Hippo signalling pathway. *Br. J. Pharmacol.* 176, 2465–2481. <https://doi.org/10.1111/bph.14674>.
  - Roehrborn, C.G., Spann, M.E., Myers, S.L., Serviss, C.R., Hu, L., and Jin, Y. (2015). Estrogen receptor beta agonist LY500307 fails to improve symptoms in men with enlarged prostate secondary to benign prostatic hypertrophy. *Prostate Cancer Prostatic Dis.* 18, 43–48. <https://doi.org/10.1038/pcan.2014.43>.
  - Pandey, D.P., Lappano, R., Albanito, L., Madeo, A., Maggolini, M., and Picard, D. (2009). Estrogenic GPR30 signalling induces proliferation and migration of breast cancer cells through CTGF. *EMBO J.* 28, 523–532. <https://doi.org/10.1038/emboj.2008.304>.
  - Yang, Y., Sheng, J., Hu, S., Cui, Y., Xiao, J., Yu, W., Peng, J., Han, W., He, Q., Fan, Y., et al. (2022). Estrogen and G protein-coupled estrogen receptor accelerate the progression of benign prostatic hyperplasia by inducing prostatic fibrosis. *Cell Death Dis.* 13, 533. <https://doi.org/10.1038/s41419-022-04979-3>.
  - Kumar, R., Verma, V., Sarswat, A., Maikhuri, J.P., Jain, A., Jain, R.K., Sharma, V.L., Dalela, D., and Gupta, G. (2012). Selective estrogen receptor modulators regulate stromal proliferation in human benign prostatic hyperplasia by multiple beneficial mechanisms—action of two new agents. *Invest. New Drugs* 30, 582–593. <https://doi.org/10.1007/s10637-010-9620-2>.
  - Glienke, W., Dolgova, Y., Müller, I., Grösch, S., Binder, J., Geisslinger, G., and Jonas, D. (2004). Induction of apoptosis in human prostate stromal cells by 4-hydroxytamoxifen: an alternative therapy for benign prostatic hyperplasia. *World J. Urol.* 22, 452–456. <https://doi.org/10.1007/s00345-004-0450-8>.
  - Luo, J., and Yu, F.X. (2019). GPCR-Hippo Signaling in Cancer. *Cells* 8, 426. <https://doi.org/10.3390/cells8050426>.
  - Wang, Z., Liu, P., Zhou, X., Wang, T., Feng, X., Sun, Y.P., Xiong, Y., Yuan, H.X., and Guan, K.L. (2017). Endothelin Promotes Colorectal Tumorigenesis by Activating YAP/TAZ. *Cancer Res.* 77, 2413–2423. <https://doi.org/10.1158/0008-5472.CAN-16-3229>.
  - Wang, J., Hong, Y., Shao, S., Zhang, K., and Hong, W. (2018). FFAR1-and FFAR4-dependent activation of Hippo pathway mediates DHA-induced apoptosis of androgen-independent prostate cancer cells. *Biochem. Biophys. Res. Commun.* 506, 590–596. <https://doi.org/10.1016/j.bbrc.2018.10.088>.
  - Dethlefsen, C., Hansen, L.S., Lillelund, C., Andersen, C., Gehl, J., Christensen, J.F., Pedersen, B.K., and Hojman, P. (2017). Exercise-Induced Catecholamines Activate the Hippo Tumor Suppressor Pathway to Reduce Risks of Breast Cancer Development. *Cancer Res.* 77, 4894–4904. <https://doi.org/10.1158/0008-5472.CAN-16-3125>.
  - Cortes, E., Lachowski, D., Rice, A., Thorpe, S.D., Robinson, B., Yeldag, G., Lee, D.A., Ghemto, L., Rombouts, K., and Del Rio Hernández, A.E. (2019). Tamoxifen

- mechanically deactivates hepatic stellate cells via the G protein-coupled estrogen receptor. *Oncogene* 38, 2910–2922. <https://doi.org/10.1038/s41388-018-0631-3>.
43. Yu, T., Yang, G., Hou, Y., Tang, X., Wu, C., Wu, X.A., Guo, L., Zhu, Q., Luo, H., Du, Y.E., et al. (2017). Cytoplasmic GPER translocation in cancer-associated fibroblasts mediates cAMP/PKA/CREB/glycolytic axis to confer tumor cells with multidrug resistance. *Oncogene* 36, 2131–2145. <https://doi.org/10.1038/onc.2016.370>.
  44. Chuang, S.C., Chen, C.H., Chou, Y.S., Ho, M.L., and Chang, J.K. (2020). G Protein-Coupled Estrogen Receptor Mediates Cell Proliferation through the cAMP/PKA/CREB Pathway in Murine Bone Marrow Mesenchymal Stem Cells. *Int. J. Mol. Sci.* 21, 6490. <https://doi.org/10.3390/ijms21186490>.
  45. Cinar, B., Al-Mathkour, M.M., Khan, S.A., and Moreno, C.S. (2020). Androgen attenuates the inactivating phospho-Ser-127 modification of yes-associated protein 1 (YAP1) and promotes YAP1 nuclear abundance and activity. *J. Biol. Chem.* 295, 8550–8559. <https://doi.org/10.1074/jbc.RA120.013794>.
  46. Schuster, G.A., and Schuster, T.G. (1999). The relative amount of epithelium, muscle, connective tissue and lumen in prostatic hyperplasia as a function of the mass of tissue resected. *J. Urol.* 161, 1168–1173.
  47. Price, H., McNeal, J.E., and Stamey, T.A. (1990). Evolving patterns of tissue composition in benign prostatic hyperplasia as a function of specimen size. *Hum. Pathol.* 21, 578–585. [https://doi.org/10.1016/s0046-8177\(96\)90002-7](https://doi.org/10.1016/s0046-8177(96)90002-7).
  48. Brennen, W.N., and Isaacs, J.T. (2018). Mesenchymal stem cells and the embryonic reawakening theory of BPH. *Nat. Rev. Urol.* 15, 703–715. <https://doi.org/10.1038/s41585-018-0087-9>.
  49. Xie, Q., Chen, J., Feng, H., Peng, S., Adams, U., Bai, Y., Huang, L., Li, J., Huang, J., Meng, S., and Yuan, Z. (2013). YAP/TEAD-mediated transcription controls cellular senescence. *Cancer Res.* 73, 3615–3624. <https://doi.org/10.1158/0008-5472.CAN-12-3793>.
  50. Xie, K., Xu, C., Zhang, M., Wang, M., Min, L., Qian, C., Wang, Q., Ni, Z., Mou, S., Dai, H., et al. (2019). Yes-associated protein regulates podocyte cell cycle re-entry and dedifferentiation in adriamycin-induced nephropathy. *Cell Death Dis.* 10, 915. <https://doi.org/10.1038/s41419-019-2139-3>.
  51. Ma, J., Chen, T., Wu, S., Yang, C., Bai, M., Shu, K., Li, K., Zhang, G., Jin, Z., He, F., et al. (2019). iProX: an integrated proteome resource. *Nucleic Acids Res.* 47, D1211–D1217. <https://doi.org/10.1093/nar/gky869>.
  52. Chen, T., Ma, J., Liu, Y., Chen, Z., Xiao, N., Lu, Y., Fu, Y., Yang, C., Li, M., Wu, S., et al. (2022). iProX in 2021: connecting proteomics data sharing with big data. *Nucleic Acids Res.* 50, D1522–D1527. <https://doi.org/10.1093/nar/gkab1081>.
  53. Surowiec, I., Koc, M., Antti, H., Wikström, P., and Moritz, T. (2011). LC-MS/MS profiling for detection of endogenous steroids and prostaglandins in tissue samples. *J. Sep. Sci.* 34, 2650–2658. <https://doi.org/10.1002/jssc.201100436>.

STAR★METHODS

KEY RESOURCES TABLE

REAGENT or RESOURCE	SOURCE	IDENTIFIER
<b>Antibodies</b>		
YAP	Cell Signaling Technology	Cat#14074; RRID:AB_2650491
YAP/TAZ	Cell Signaling Technology	Cat#93622; RRID:AB_2904489
Phospho-YAP (Ser127)	Cell Signaling Technology	Cat#13008; RRID:AB_2650553
Phospho-TAZ (Ser89)	Cell Signaling Technology	Cat#59971; RRID:AB_2799578
CDK4	Cell Signaling Technology	Cat#12790; RRID:AB_2631166
CDK6	Cell Signaling Technology	Cat#13331; RRID:AB_2721897
Bax	Cell Signaling Technology	Cat#2772; AB_10695870
Bcl-2	Cell Signaling Technology	Cat#15071; RRID:AB_2744528
LATS1	Cell Signaling Technology	Cat#3477; RRID:AB_2133513
LATS2	Cell Signaling Technology	Cat#5888; RRID:AB_10835233
Phospho-LATS1 (Ser909)	Cell Signaling Technology	Cat#9157; RRID:AB_2133515
MST1	Cell Signaling Technology	Cat#3682; RRID:AB_2144632
MST2	Cell Signaling Technology	Cat#3952; RRID:AB_2196471
Phosphor-MST1/MST2 (Thr180/183)	abcam	Cat#ab76323; RRID:AB_1523982
GPER	abcam	Cat#ab39742; RRID:AB_1141090
CREB	abcam	Cat#ab178322; RRID:AB_2827810
Anti-rabbit Alexa Fluor 488	abcam	Cat# ab150077; RRID:AB_2630356
Phosphor-CREB (Ser133)	Immunoway	Cat#YP0075; RRID:AB_3064815
Anti-mouse IgG-HRP	Immunoway	Cat#RS0001; RRID:AB_2943495
Anti-rabbit IgG-HRP	Immunoway	Cat#RS0002; RRID:AB_2943496
Cyclin D1	Proteintech	Cat#60186-1-Ig; RRID:AB_10793718
β-Tubulin	Proteintech	Cat#10094-1-AP; RRID:AB_2210695
GAPDH	Proteintech	Cat#60004-1-Ig; RRID:AB_2107436
<b>Bacterial and virus strains</b>		
pLV-MCS-3FLAG-YAP-SV40-EGFP-IRES-puromycin	GeneChem	N/A
<b>Biological samples</b>		
Human prostate tissues diagnosed with benign prostatic hyperplasia	Peking University First Hospital (Beijing, China)	N/A
<b>Chemicals, peptides, and recombinant proteins</b>		
Verteporfin (VP)	Selleck	Cat#S1786
Estradiol (E <sub>2</sub> )	Selleck	Cat#S1709
G-1	Selleck	Cat#S0851
G-15	Selleck	Cat#S6651
4-hydroxytamoxifen (OHT)	Selleck	Cat#S8956
H 89 2HCl (H89)	Selleck	Cat#S1582
DAPI	Solarbio	Cat#C0065
Puromycin	Solarbio	Cat#P8230
Lipofectamine RNAiMAX Transfection Reagent	Invitrogen	Cat#13778075
TRlzol	Invitrogen	Cat#15596018CN

(Continued on next page)

**Continued**

REAGENT or RESOURCE	SOURCE	IDENTIFIER
PageRuler Prestained Protein Ladder	Thermo Scientific	Cat#26616
Immobilon Western HRP Substrate	Millipore	Cat#WBKLS0500
<b>Critical commercial assays</b>		
EasyScript First-Strand cDNA Synthesis SuperMix	TransGen	Cat#AE301-02
TransStart Top Green qPCR SuperMix	TransGen	Cat#AQ131-01
CCK-8 kit	KeyGEN	Cat#KGA317-2
Cell Cycle kit	KeyGEN	Cat#KGA512
Cell apoptosis Kit	KeyGEN	Cat# KGA108
<b>Deposited data</b>		
iTRAQ-based LC-MS/MS analysis raw data	This paper	PXD048857
Original western blot data/Data S1 (deposited on Mendeley)	This paper	<a href="https://doi.org/10.17632/nz5zh5vvy7.1">https://doi.org/10.17632/nz5zh5vvy7.1</a>
<b>Experimental models: Cell lines</b>		
Human: BPH-1	KeyGEN	Cat#KG1008; RRID:CVCL_1091
Human: RWPE-1	ATCC	Cat#CRL-3607; RRID:CVCL_3791
<b>Oligonucleotides</b>		
siRNA for YAP	RiboBio	Cat#SIGS0003678-1
Primers for YAP, TAZ, CTGF, CYR61, EDN1, EGR1, ANKRD1, GPER, GAPDH, see Table S2	Sangon	N/A
<b>Software and algorithms</b>		
ImageJ	ImageJ	<a href="https://imagej.nih.gov/ij/">https://imagej.nih.gov/ij/</a>
Flowjo 10	Becton, Dickinson & Company	<a href="https://www.flowjo.com/">https://www.flowjo.com/</a>
LAS X	Leica	<a href="https://www.leica-microsystems.com/products/microscope-software/p/leica-las-x-ls/">https://www.leica-microsystems.com/products/microscope-software/p/leica-las-x-ls/</a>
SPSS 24.0	IBM	<a href="https://www.ibm.com/cn-zh/spss">https://www.ibm.com/cn-zh/spss</a>
Graphpad Prism 8.0	Graphpad	<a href="https://www.graphpad-prism.cn/">https://www.graphpad-prism.cn/</a>
BioRender	BioRender	<a href="https://www.biorender.com/">https://www.biorender.com/</a>

**RESOURCE AVAILABILITY**

**Lead contact**

Information and requests for resources should be directed to and will be fulfilled by the lead contact, Dr. Jin Jie ([jinjie@vip.163.com](mailto:jinjie@vip.163.com)).

**Materials availability**

This study did not generate any new unique reagents.

**Data and code availability**

- Data: The iTRAQ-based LC-MS/MS analysis raw data reported in this paper have been deposited in the ProteomeXchange Consortium via the iProX<sup>51,52</sup> partner repository with the project ID PXD048857. All relevant data are available from the [lead contact](#) upon request.
- Code: This paper does not report original code.
- Any additional information required to re-analyze the data reported in this paper is available from the [lead contact](#) upon request.

**EXPERIMENTAL MODEL AND STUDY PARTICIPANT DETAILS**

**Patients and tissue samples**

Thirty-two prostate tissues were obtained from Peking University First Hospital (Beijing, China), and the diagnosis was confirmed by two experienced pathologists. Patients who underwent transurethral resection of the prostate (TURP) were included in this study, but those with

prostate cancer, prostatitis and urinary catheter insertions were excluded; those treated with alpha-adrenergic receptor antagonists or 5 $\alpha$ -reductase inhibitors were also excluded. All retrospective clinical data analyses and prostate specimen collection procedures were performed after obtaining informed consent from all patients and approval from the Peking University First Hospital Institutional Review Board. Patient information is included in [Table S1](#). Prostate tissues obtained from patients post-surgery were allocated into four categories: one for proteomic analysis, one for detecting endogenous steroids, one fixed overnight in 10% formalin buffer for subsequent staining analysis, and the last stored in liquid nitrogen.

### Cell culture and transfection

The BPH-1 cell line was purchased from KeyGEN (KG1008, KeyGen Biotech Co., Ltd., NJ, China) and cultured in Roswell Park Memorial Institute (RPMI)-1640 medium with 10% fetal bovine serum (Gibco) supplemented with 1% penicillin and streptomycin. The RWPE-1 cell line was purchased from the American Type Culture Collection and cultured in complete keratinocyte serum-free medium (Invitrogen, USA). All cells were cultured in a humidified atmosphere with 5% CO<sub>2</sub> maintained at 37°C and tested for mycoplasma on a regular basis. All cell lines were regularly tested for mycoplasma contamination using the LookOut Mycoplasma PCR Detection Kit (Sigma).

For overexpression of YAP, recombinant pLV-MCS-3FLAG-YAP-SV40-EGFP-IRES-puromycin, the corresponding control plasmid vectors and the lentivirus were produced by Shanghai GeneChem Co., Ltd. The stable cell line was established by lentivirus infection according to the multiplicity of infection (MOI) value. The stable YAP-overexpressing BPH-1 cell line was selected with puromycin (1  $\mu$ g/mL).

## METHOD DETAILS

### iTRAQ-based LC-MS/MS

Each tissue sample was homogenized with RIPA buffer (50 mM Tris-HCl, pH 7.4; 100 mM NaCl; 1 mM PMSF; 1 mM EDTA; 1% Triton X-100; 1% sodium deoxycholate; and 2% SDS). A bicinchoninic acid (BCA) assay was performed to quantify the protein concentration in each sample. The proteins were digested with trypsin and incubated at 37°C overnight. iTRAQ reagents were used to label peptides generated in accordance with the protocols of the manufacturer of an 8-plex iTRAQ Multiplex kit (AB Sciex, Framingham, MA). Using the Easy nLC/Ultimate 3000 system (Thermo Scientific, USA), the labeled peptide mixtures were separated. Mass spectra were recorded on a Q Exactive mass spectrometer configured with a Nano-ESI source (Thermo Scientific, USA). Protein identification was performed using the MASCOT search engine (version 2.4.1; Matrix Science, London, UK) embedded in Proteome Discoverer 1.3 (Thermo Electron, San Jose, CA, USA). Totally 2433 proteins were analyzed. *p* value less than 0.05 and the fold change ratio  $\geq 1.5$  or  $\leq 0.8$  were set as the threshold for DEPs.

### Hormone analysis

E<sub>2</sub>, DHT, T, A-dione and P were measured by LC-MS/MS. The assay was adapted from that described by Surowiec et al.<sup>53</sup> Prostate samples were immediately frozen in liquid nitrogen and stored at  $-80^{\circ}\text{C}$  until analysis after collected at the Peking University First Hospital. For analysis of hormones in prostate, 500  $\mu$ L of methanol with hormones of specific concentrations as an internal standard was added to 100mg tissue. Standard solutions of all hormones were prepared in methanol as external standard. The mixture was homogenized using a vibration mill with 2 tungsten carbide beads (diameter, 3mm) at a frequency of 30Hz for 2min. After extraction the methanol solution was centrifuged at 14 000rpm for 15 min at 4°C and the supernatant was kept at  $-80^{\circ}\text{C}$  awaiting LC-MS/MS analysis.

### Immunohistochemistry and immunofluorescence

The TURP-operated prostate tissue was fixed overnight in 10% formalin buffer at 4°C, dehydrated, and conventionally embedded in paraffin. Then, the sections were cut into 5  $\mu$ m sections. After dewaxing, hydration, and heat-induced epitope retrieval, 3% hydrogen peroxide was used to inactivate endogenous peroxidase. Non-specific binding was blocked by incubating sections in serum. Primary antibodies were incubated overnight at 4°C. Anti-YAP (1:400) and anti-GPER (1:500) antibodies were used for staining. Sections incubated with secondary antibodies in the absence of primary antibodies were used as negative controls. All analyses were performed by two experienced pathologists in a blinded fashion. Each slice was selected from five random 200-fold visual horizons for observation, and the staining results were recorded. Image-Pro Plus 6.0 and ImageJ software was used for further quantification of DAB intensity and the percentage of staining area. The intensity and staining area values for epithelial YAP and GPER were classified into corresponding groups based on the following scoring system: 0 (negative staining), 1 (weak staining), 2 (moderate staining), and 3 (strong staining).

For immunofluorescence, BPH-1 cells were seeded on glass coverslips and treated with the corresponding agents. Sections were then incubated with the primary antibody against YAP followed by incubation with the secondary antibody, Alexa Fluor 488-labeled goat anti-rabbit IgG (1:1000; abcam), for detection. DAPI (Solarbio) was used to identify cell nuclei, and fluorescence was detected with a TCS SP8 MP FLIM system (Leica). Fluorescence intensity of each observation was quantified by ImageJ software.

### RNAi

Synthetic siRNA oligonucleotides were synthesized by RiboBio (Guangzhou, China). Transfection of the siRNAs using RNAiMAX (Invitrogen, Carlsbad, CA, USA) was performed according to the manufacturer's instructions.

### RNA extraction and quantitative real-time PCR (qRT-PCR)

Total RNA from treated cells was isolated using TRIzol reagent (Invitrogen). Total RNA (1 µg) was reverse transcribed into cDNA using EasyScript First-Strand cDNA Synthesis SuperMix (TransGen Biotech) according to the manufacturer's instructions. PCR amplification of the resulting cDNA templates was conducted using the following conditions in forty cycles: denaturation at 94°C for 30 s, annealing at 60°C for 45 s and extension at 72°C for 30 s. PCR products were separated on a 1.5% agarose gel and visualized by staining with ethidium bromide. Real-time PCRs were performed using TransStart Top Green qPCR SuperMix (TransGen Biotech) for a two-step cycling protocol on a 7500 Fast Real-Time PCR System (ABI). Relative expression levels were calculated using the  $2^{-\Delta\Delta C_t}$  method. Primer for q-RT PCR analysis see [Table S2](#).

### Western blot analysis

Adherent cells were rinsed with ice-cold PBS and removed from the dish using a cell scraper. RIPA buffer, supplemented with freshly added protease and phosphatase inhibitors, was employed for cell lysis. The lysate underwent centrifugation at a high speed (12,000g) for 15 min at 4°C, and the resultant supernatant was carefully collected. The protein concentration was quantified using a BCA protein assay. SDS-PAGE and Western blotting were carried out following standard protocols. Thermo Scientific PageRuler Prestained Protein Ladder was applied as protein ladder. The NC membranes were blocked with 5% skim milk and incubated overnight at 4°C with the primary antibodies, which are described in the Chemicals and antibodies section. Then, the membranes were incubated with the appropriate secondary antibodies (1:5000; Abcam, USA) and visualized with enhanced chemiluminescence using an ECL kit (Millipore). Western blot bands were exposed to X-ray films and quantified by Genesys software. The relative expression of protein was standardized by comparison with anti-GAPDH or anti-β-tubulin antibody. All primary antibodies used in this work were appropriately diluted at 1:1000. All the western blot results from this experiment were included in the supplementary data ([Data S1](#)), which contains images of all original western blots, encompassing three experimental replicates.

### CCK-8 cell proliferation assay

Cell proliferation was determined with a CCK-8 kit (KeyGEN) according to the manufacturer's instructions. A total of 1000 cells/well were seeded in a 96-well flat-bottomed plate. After the cells adhered to the well, the culture medium was replaced with the corresponding treatment. Cell proliferation was detected every 24 h for 4 successive days. At each time point, 10 µL of CCK-8 reagent was added to each well, and the cells were incubated at 37°C for 3 h. The absorbance was finally detected at a wavelength of 450 nm with a microplate reader (Thermo Scientific, USA). Experiments were repeated at least three times.

### Flow cytometry analysis

For cell cycle assessment, prostate epithelial cell lines (RWPE-1 and BPH-1 cell lines) were seeded on a six-well cell culture plate and treated with VP(250 nM, 500 nM), G1 (1 µM), E<sub>2</sub> (10 nM) or siNC, siYAP (final concentration of 100 nM) for 48 h. The cells were collected and fixed in 70% cold ethanol overnight at 4°C and then incubated with RNase A at 37°C for 60 min in the dark and subsequently stained with propidium iodide (PI) (KeyGen) staining solution. The samples were immediately analyzed on a FACSsort flow cytometer (FACS Calibur, Becton Dickinson). The data were processed by FlowJO software.

Cell apoptosis was assayed by staining with Annexin V-FITC and PI (KeyGEN) following the manufacturer's instructions and detected with a flow cytometer (FACS Calibur, Becton Dickinson). Cells without staining or Annexin V-FITC and PI double staining were tested to adjust voltage and compensation before collecting data. Prostate epithelial cell lines (RWPE-1 and BPH-1 cell lines) were seeded on a six-well cell culture plate, and after the adherent cells reached 50–60% confluency, they were treated with the corresponding reagents for 48h. Experiments were repeated at least three times.

### QUANTIFICATION AND STATISTICAL ANALYSIS

In this study, all data were statistically analyzed using SPSS 24.0 and GraphPad Prism 8.0 software. Each experiment was repeated at least three times, and the measurement data are expressed as the means ± standard deviation. All continuous variables were compared between groups using t-tests and analysis of variance (ANOVA), and all discrete variables were compared between groups using nonparametric tests (Mann-Whitney test). Pearson's correlation analysis and Chi-square test were applied to determine whether there is a significant association between two variables.  $p < 0.05$  was considered to be statistically significant.